The Journal of Physical Chemistry B

 VOLUME 103, NUMBER 11, MARCH 18, 1999

LETTERS

X-ray Reflectivity Study of the Water−Hexane Interface

Dragoslav M. Mitrinovic,[†] Zhongjian Zhang,[†] Scott M. Williams,[†] Zhengqing Huang,[‡] and Mark L. Schlossman*[,†,§]

Department of Physics, University of Illinois at Chicago, 845 West Taylor Street, Chicago, Illinois 60607, Brookhaven National Laboratory, National Synchrotron Light Source, Upton, New York 11973, and Department of Chemistry, University of Illinois at Chicago, 845 West Taylor Street, Chicago, Illinois 60607

Received: December 4, 1998

Synchrotron X-ray reflectivity is used to study the electron density profile normal to the bulk water−hexane interface. This first measurement of the microscopic interfacial width of a neat water−oil interface relied upon the development of a novel technique to flatten the liquid−liquid interface. The measurement is interpreted in terms of an error function electron density profile to yield an interfacial width of 0.33 ± 0.025 nm. Within the context of capillary wave theory, it is shown that this microscopic parameter is in agreement with macroscopic measurements of the interfacial tension. These measurements are compared to computer simulations of water−alkane interfaces.

Introduction

An outstanding problem in the area of interfacial phenomena is the determination of structure at liquid−liquid interfaces. This structure is relevant, for example, to the understanding of electron and molecular transfer across biological membranes and to the partitioning of solvents and metal ions across liquid−liquid interfaces. Liquid−liquid interfaces can be viewed also as model systems whose study will influence our understanding of inhomogeneous materials. The experimental characterization of interfaces can provide an important reference for computer simulations of interfaces that depend sensitively upon the intermolecular potentials.[1,2] In spite of their importance, fundamental questions remain in the study of liquid−liquid interfaces that have been barely addressed. There is currently a poor understanding of electron and molecular density profiles both normal to the interface and within the plane of the interface.

Of fundamental importance in the study of liquid−liquid interfaces is the interface between two pure liquids such as water and alkane. Molecular dynamics simulations have focused upon the issues of the interfacial width and orientational order close to the interface. For example, Carpenter and Hehre used molecular dynamics to study the water−hexane interface.[1] They found an interfacial 90−10 width of 1.0 ± 0.3 nm that described a diffuse interface (the 90−10 width is defined as the distance required for the water density to drop from 90% to 10% of its bulk value). Other molecular dynamics simulations found that the interface sharpness depends sensitively upon the intermolecular potentials.[2] These simulations are important not only for improving our understanding of the interfacial structure, but also for identifying appropriate intermolecular potentials.

Unfortunately, simulations and other theoretical work on neat liquid−liquid interfaces (without surfactants) have been handicapped by a lack of experimental data on the microscopic structure of these interfaces. Although precise measurements of the interfacial tension have been conducted over a period of many years,[3] there are few experimental techniques capable of directly probing the order on the molecular length scale at this

* Author to whom correspondence should be addressed. E-mail: schloss@uic.edu.
[†] Department of Physics, University of Illinois at Chicago.
[‡] Brookhaven National Laboratory.
[§] Department of Chemistry, University of Illinois at Chicago.

10.1021/jp984640o CCC: $18.00
Published on Web 02/27/1999

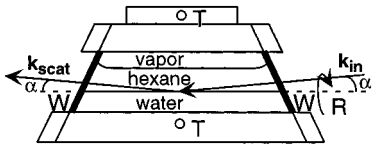

Figure 1. Cross-sectional view of sample cell; W = Mylar windows; T = thermistor to measure temperature; R = rotation about the horizontal used to fine tune the sample flatness. The kinematics of surface X-ray reflectivity is also indicated: $\mathbf{k}_{in}$ is the incoming X-ray wave vector, $\mathbf{k}_{scat}$ is the scattered wave vector, α is the angle of incidence and reflection.

interface. Nonlinear optical probes are a recently developed, notable exception that provide information about molecular conformations.[4−7] A reflection second-harmonic generation measurement by Conboy et al. probed the orientational ordering of *n*-alkanes at the water−alkane interface.[5] Although this technique has not been used to study the interfacial width, two other techniques—X-ray and neutron reflectivity—have been used to study the interfacial width at the water−*vapor* interface.[8−10] Until now, technical difficulties have prevented the use of X-ray and neutron reflectivity in the study of neat liquid−liquid interfaces such as the water−alkane interface.

Although several groups have recently applied X-ray or neutron surface scattering to the study of liquid−liquid interfaces, these measurements were limited to the study of special interfacial conditions. These included either the use of upper liquid phases that wet the lower phase or interfaces of ultralow interfacial tension.[11−15] However, many common and important liquid−liquid interfaces consist of nonwetting liquids with interfacial tensions on the order of 1−50 mN/m. The higher tension of an interface such as the water−hexane interface results in a macroscopically curved interface. This curvature has, in the past, precluded the use of X-ray scattering to investigate the interfacial structure in the majority of liquid−liquid systems.

The primary difficulty for X-ray studies of liquid−liquid interfaces is that the macroscopically curved interface alters the profile of the scattered X-ray beam, severely complicating both measurements and data analysis. We present a simple and general technique to flatten a liquid−liquid interface to an extent sufficient for X-ray surface scattering measurements. The interfacial width of the water−hexane interface is then measured with X-ray reflectivity. Capillary wave theory allows us to relate the microscopic width parameter determined by X-ray reflectivity to the interfacial tension determined by conventional macroscopic measurements.[9,16,17]

Experimental Methods

The measurements presented here are from samples first stirred with a Teflon-coated stir bar and allowed to reach thermal equilibrium in a vapor−tight sample cell (Figure 1). High-purity water was produced from a Barnstead NanoPure system; *n*-hexane (99+%) was purchased from Sigma. The liquids were contained in a polycarbonate sample cell with Mylar X-ray windows and Mylar wall inserts arranged such that the liquid−liquid interface was in contact only with Mylar. The interfacial area was 76 mm × 100 mm (along the beam *x* transverse) with X-rays penetrating through the upper phase (see Figure 1). At the chosen X-ray wavelength the absorption lengths for hexane and water are 19.2 and 5.6 mm, respectively. The sample cell is contained in a one-stage cylindrical aluminum thermostat with X-ray windows made from Kapton. The thermostat is temperature controlled to ±0.03 °C using Minco adhesive heaters, a control thermistor, and a Lakeshore 340 temperature controller.

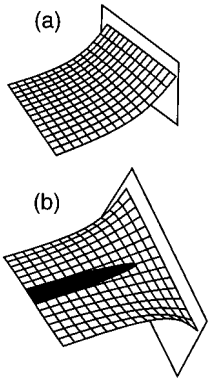

Figure 2. Cartoon of a liquid−liquid interface: (A) before twisting, (B) after twisting. The checkerboard represents part of the interface; the rectangles are the sample cell windows; the dark region is a partial X-ray footprint. The position of the line of the interface in contact with the window is pinned and does not change as the sample is rotated.

Two thermistors mounted within the polycarbonate sample cell immediately above and below the liquid chamber measure the sample temperature and allow us to determine when the sample cell has thermally equilibrated.

The sample cell windows were slanted 25° from the vertical to reduce the curvature of the interface (Figure 1). This curvature is due to the contact angle of the meniscus where the water−hexane interface is in contact with the windows of the sample cell. However, due to the nonequilibrium nature of these contact angles and the stringent requirement for flatness posed by X-ray reflectivity, fine tuning of the interface flatness is required beyond that obtained by slanting the cell windows. An interface is flat enough for X-ray reflectivity measurements if the divergence of the reflected X-rays is smaller than the detector angular resolution (typically 10^{-3} to 10^{-4} rad) required for the particular system under study.

A general solution to flatten the interface takes advantage of the nonequilibrium nature of a pinned meniscus. Except for specially prepared microscopically flat surfaces, contact angles exhibit hysteresis due to surface roughness.[18] To enhance the pinning of the liquids, the Mylar windows were roughened slightly by rubbing with polyethylene gloves. With the liquid−liquid interface meniscus pinned to the cell windows, the sample cell can be rotated about a horizontal axis to twist the entire interface. This results in a strip of interface that is very flat (Figure 2). With adequate sample flatness, the X-ray reflectivity is constant as the X-ray beam is scanned across the interface at a fixed angle of incidence. This indicates that the beam is reflected at the same reflection angle for different parts of the interface. Also, the reflectivity is nearly 100% when the incident beam is below the angle for total reflection. All of our measurements were taken from samples that passed these two tests.

X-ray reflectivity was conducted at beamline X19C at the National Synchrotron Light Source (Brookhaven National Laboratory) with a liquid surface spectrometer and measurement techniques described in detail elsewhere.[14] The kinematics of reflectivity is illustrated in Figure 1; note that α = 90° is normal to the surface. For specular reflection, the wave vector transfer, $\boldsymbol{Q} = \mathbf{k}_{scat} - \mathbf{k}_{in}$, is only in the z-direction, normal to the interface; $Q_x = Q_y = 0$, where *x* and *y* are in the plane of the interface, and $Q_z = (4\pi/\lambda)\sin(\alpha)$, where $\lambda = 0.0825 \pm 0.0002$ nm is the X-ray wavelength for these measurements.

To set the incident beam size and reduce the vertical divergence to 20 μrad, two slits placed approximately 60 cm apart were used immediately prior to the liquid sample. The

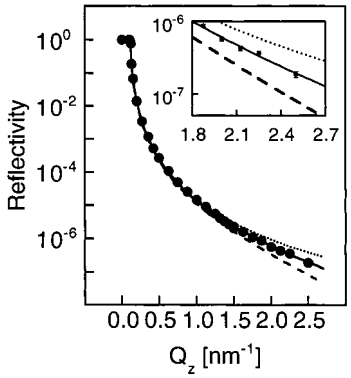

Figure 3. X-ray reflectivity from the water−hexane interface as a function of wave vector transfer normal to the interface: (●) measurements at 32.00 °C; (—) fit described in the text; (···) Fresnel reflectivity for ideal interface; (- - -) prediction from molecular dynamics simulation of Carpenter and Hehre. The inset is an expanded view of the high Q_z region. Error bars on the data are similar to the symbol size in the inset.

slit gaps were typically 5−10 μm in the vertical at the smallest reflection angles (horizontal slit gaps were 10 mm, much larger than the horizontal beam size of ∼2 mm). A scintillator monitor immediately prior to the sample measured the incident X-ray flux. The sample was followed by a slit with a vertical gap of ∼2 mm to reduce the background scattering, and the scintillator detector was preceded immediately by a slit with a vertical gap of 400 μm which set the detector resolution.

Data and Analysis

X-ray reflectivity measurements as a function of the reflection angle from a bulk interface can be analyzed to yield an electron density profile along the normal to the interface (and averaged over the plane of the interface) with a resolution of a fraction of a nanometer.[19] Figure 3 illustrates the X-ray reflectivity, $R(Q_z)$, measured from the water−hexane interface at 32.00 °C.[20] The reflectivity varies with the angle of reflection, α, expressed here in terms of the wave vector transfer normal to the interface, $Q_z = (4\pi/\lambda)\sin\alpha$. Also shown is the Fresnel reflectivity, $R_F(Q_z)$, predicted for an ideal, smooth, and flat interface.[21] Both of these curves have a small region of constant reflectivity (equal to 1) below a critical wave vector transfer, $Q_c = 0.123$ nm^{-1}, corresponding to a region of total reflection. Both curves then drop off rapidly and smoothly with increasing wave vector transfer.

Although the qualitative features of the ideal and measured curves are similar, the reduction in intensity of the measured reflectivity at larger wave vector transfer is the result of X-rays being scattered by interfacial roughness due to thermally induced capillary wave fluctuations. The classical capillary wave model for the fluctuations[22] corresponds to an error function profile for the electron density averaged over the plane of the interface, $\langle\rho(z)\rangle$, given by

$$\langle\rho(z)\rangle = \frac{1}{2}(\rho_w + \rho_h) + \frac{1}{2}(\rho_w - \rho_h)erf[z/\sigma\sqrt{2}]$$
$$\text{with } erf(z) = \frac{2}{\sqrt{\pi}}\int_0^z e^{-t^2}\,dt \quad (1)$$

where $\rho_{w,h}$ represent the electron densities (normalized to the value for water) of bulk water ($\rho_w = 1$) and hexane ($\rho_h = 0.68$) and σ is the interfacial width. For this interfacial profile, the distorted wave Born approximation expresses the ratio of the measured reflectivity to the Fresnel reflectivity as[23,24]

$$\frac{R(Q_z)}{R_F(Q_z)} \cong \exp(-Q_z Q_z^T \sigma^2) \quad (2)$$

where $Q^T_z \cong \sqrt{Q_z^2 - Q_c^2}$ is the z-component of wave vector transfer with respect to the lower phase and Q_c is the critical wave vector transfer for total reflection of the X-rays from the lower phase. More explicitly, the reflected intensity in eq 2 can be written as

$$R(Q_z) \cong \left|\frac{Q_z - Q_z^T}{Q_z + Q_z^T}\right|^2 \exp(-Q_z Q_z^T \sigma^2) \quad (3)$$

A fit of the data to eq 3 using a single fitting parameter, σ, is illustrated by the solid line in Figure 3 and yields the interfacial width $\sigma = 0.33 \pm 0.025$ nm. The accuracy of this fit is limited by the range of Q_z. The highest Q_z obtainable is limited primarily by the background scattering from the bulk liquid, which is measured and subtracted from the reflected intensity.

Discussion

In addition to the capillary wave contribution just discussed, the interfacial width may also contain a contribution from an intrinsic profile described, for example, by van der Waals theories.[25] In the spirit of a hybrid model of the interface that describes this intrinsic profile roughened by capillary waves, the total interfacial width, σ_{total}, can be represented as a combination of an intrinsic profile width, σ_o, and the capillary wave contribution[8,9,16,17,26] where k_BT is Boltzmann's constant

$$\sigma^2_{total} = \sigma_o^2 + \frac{k_B T}{2\pi\gamma}\int_{q_{min}}^{q_{max}} \frac{q\,dq}{q^2 + \xi_{||}^{-2}} \equiv \sigma_o^2 + \sigma_{cap}^2 \quad (4)$$

times the temperature, γ is the interfacial tension, the correlation length, $\xi_{||}$, is given by $\xi^2_{||} = \gamma/\Delta\rho_m g$ and determines the exponential decay of the interfacial correlations given by the height−height correlation function of interfacial motion,[27] $\Delta\rho_m$ is the *mass* density difference of the two phases, and g is the gravitational acceleration. The wave vector, q, represents the in-plane capillary waves. The limit q_{min} is determined by the instrumental resolution that sets the largest in-plane capillary wavelength that the measurement probes. The limit, q_{max}, is determined by the cutoff for the smallest wavelength capillary waves that the interface can support. Direct calculation of σ_{cap} using the literature value of the interfacial tension (51.4 mN/m at $T = 22$ °C)[3] and $q_{max} = 2\pi/0.5$ nm^{-1} yields $\sigma_{cap} = 0.329$ nm, in agreement with our measurement of $\sigma = 0.33$ nm. This indicates that the intrinsic profile width, σ_o, is small for this interface.

Alternatively, eq 4 (with $\sigma_o = 0$) can be used to predict a value of the interfacial tension, γ, from the measured interfacial width. This is done by comparing this measurement at the water−hexane interface to an earlier measurement at the water−vapor interface.[9] For these two particular experiments, we expect that the value of the integral in eq 4 is essentially the same. Therefore, eq 4 leads to $\sigma^2_{w-v}\gamma_{w-v}/k_BT_{w-v} \cong \sigma^2_{w-h}\gamma_{w-h}/k_BT_{w-h}$ (where $\gamma_{w-v} = 72.5$ mN/m and $\sigma_{w-v} = 0.27$ nm at $T_{w-v} = 20$ °C).[9,28] The interfacial tension at the water−hexane interface predicted from our measurement is $\gamma_{w-h} = 51.9 \pm 5$ mN/m at $T = 32$ °C, in agreement with the literature value of 51.4 mN/m (at $T = 22$ °C) measured by a tensiometer or the pendant drop technique.[3]

The measured value of the interfacial width for the water−hexane interface can be compared to recent predictions from

molecular dynamics simulations for water−alkane interfaces: 0.39 ± 0.12 nm for water−hexane,[1] 0.12 nm for water−octane,[29] 0.15 nm for water−nonane,[30] and 0.17 nm for water−decane[2] (these values have been modified so they can be compared with the σ in our error function profile in eq 1, for example the 90−10 width is related to σ by $w_{90-10} \cong 1.82\sqrt{2}\sigma$). The simulation cells have interfacial areas of typically $(3\text{ nm})^2$ and, therefore, contain only a small part of the capillary wave spectrum probed by our reflectivity measurements. The capillary wave contribution to the interfacial width for this simulation cell size can be estimated to be 0.15 nm (using $q_{\min} = 2\pi/3\text{ nm}^{-1}$ and $q_{\max} = 2\pi/0.5\text{ nm}^{-1}$ in eq 4). Except for the simulation of the water−hexane interface, the interfacial width in these simulations can be accounted for by capillary waves alone, in agreement with our experiment on the water−hexane interface.

Only the interfacial width of the water−hexane simulation is larger than expected from capillary waves. The simulation result could be justified by postulating an intrinsic profile with $\sigma_o = 0.36$ nm. When extrapolated to a hypothetical simulation cell size that includes all the capillary waves measured by our experiment, this simulation then predicts a width of 0.49 nm, significantly larger than our experimental value of 0.33 ± 0.025 nm (see Figure 3). This discrepancy may indicate that a change of the molecular interaction parameters is needed to appropriately model this interface. For example, Buuren et al. showed that the interfacial width can be decreased by decreasing the well depth of the Lennard−Jones interaction potential between the carbon atoms of the alkane and the oxygen atoms of the water, ϵ_{C-O}.[2] This change would also reduce the solubility of hexane in water, possibly removing an anomaly in the Carpenter and Hehre simulations. Carpenter and Hehre had found a small number of hexane molecules in the region of bulk water, an observation inconsistent with the known solubility of hexane in water (as noted by the authors).

The good agreement of the interfacial tension predicted from our measurement of the microscopic interfacial width and the macroscopically determined interfacial tension establishes the soundness of these techniques in studying a simple liquid−liquid interface. This will allow us to use X-ray reflectivity to study directly the molecular length scale ordering of condensed matter phases of surfactants adsorbed at liquid−liquid interfaces. Comparison to the ordering of the same surfactants at the liquid−vapor interface will provide insight into the role of a solvent or liquid spectator phase in the formation of surfactant assemblies.[31,32]

Acknowledgment. This work was supported by the donors of the Petroleum Research Fund administered by the ACS, the UIC Campus Research Board, and the NSF Division of Materials Research. Brookhaven National Laboratory is supported by the U.S. Department of Energy.

References and Notes

(1) Carpenter, I. L.; Hehre,W. J. *J. Phys. Chem.* **1990**, *94*, 531.

(2) Buuren, A. R. v.; Marrink, S.-J.; Berendsen, H. J. C. *J. Phys. Chem.* **1993**, *97*, 9206.

(3) Goebel, A.; Lunkenheimer, K. *Langmuir* **1997**, *13*, 369.

(4) Grubb, S. G.; Kim, M. W.; Rasing, T.; Shen, Y. R. *Langmuir* **1988**, *4*, 452.

(5) Conboy, J. C.; Daschbach, J. L.; Richmond, G. L. *Appl. Phys. A.* **1994**, *59*, 623.

(6) Richmond, G. L. *Anal. Chem.* **1997**, *69*, 536A.

(7) Naujok, R. R.; Higgins, D. A.; Hanken, D. G.; Corn, R. M. *J. Chem. Soc., Faraday Trans.* **1995**, *91*, 1411.

(8) Braslau, A.; Deutsch, M.; Pershan, P. S.; Weiss, A. H.; Als-Nielsen, J.; Bohr, J. *Phys. Rev. Lett.* **1985**, *54*, 114.

(9) Schwartz, D. K.; Schlossman, M. L.; Kawamoto, E. H.; Kellogg, G. J.; Pershan, P. S.; Ocko, B. M. *Phys. Rev. A* **1990**, *41*, 5687.

(10) Penfold, J.; Thomas, R. K. *J. Phys. Condens. Matter* **1990**, *2*, 1369.

(11) Lee, L. T.; Langevin, D.; Farnoux, B. *Phys. Rev. Lett.* **1991**, *67*, 2678.

(12) Phipps, J. S.; Richardson, R. M.; Cosgrove, T.; Eaglesham, A. *Langmuir* **1993**, *9*, 3530.

(13) McClain, B. R.; Lee, D. D.; Carvalho, B. L.; Mochrie, S. G. J.; Chen, S. H.; Litster, J. D. *Phys. Rev. Lett.* **1994**, *72*, 246.

(14) Schlossman, M. L.; Synal, D.; Guan, Y.; Meron, M.; Shea-McCarthy, G.; Huang, Z.; Acero, A.; Williams, S. M.; Rice, S. A.; Viccaro, P. J. *Rev. Sci. Instrum.* **1997**, *68*, 4372.

(15) Williams, S. M.; Zhang, Z.; Mitrinovic, D.; Huang, Z.; Schlossman, M. L. Manuscript in preparation.

(16) Braslau, A.; Pershan, P. S.; Swislow, G.; Ocko, B. M.; Als-Nielsen, J. *Phys. Rev. A* **1988**, *38*, 2457.

(17) Schlossman, M. L. Surfaces and Interfaces of Fluids, Structure of; In *Encyclopedia of Applied Physics*; Trigg, G. L., Ed.; VCH Publishers: New York, 1997; Vol. 20, pp 311−336.

(18) Adamson, A. W. *Physical Chemistry of Surfaces*, 5th ed.; John Wiley & Sons: New York, 1990.

(19) Pershan, P. S. *Faraday Discuss. Chem. Soc.* **1990**, *89*, 231.

(20) The path length of the X-rays through the upper liquid phase varies as a function of the reflection angle, α, measured from the plane of the interface. Therefore, the absorption of the X-rays by the upper phase varies with the angle α. This small variation is included in the analysis of all the data sets from the liquid−liquid interface by multiplying the measured reflectivity by the factor $\exp[-\mu D\{1 - \sin 65°/\sin(65° + \alpha)\}]$, where $1/\mu$ is the X-ray absorption length in hexane, $D = 76$ mm is the length of the interface, and 65° is the angle from the horizontal of the sample cell window (see Figure 1). This small correction is approximately 3% at $Q_z = 2.5\text{ nm}^{-1}$ or $\alpha = 0.94°$.

(21) Born, M.; Wolf, E. *Principles of Optics*, 6th ed.; Pergamon Press: Oxford, 1980.

(22) Buff, F. P.; Lovett, R. A.; Stillinger, F. H. *Phys. Rev. Lett.* **1965**, *15*, 621.

(23) Nevot, L.; Croce, P. *Rev. Phys. Appl.* **1980**, *15*, 761.

(24) Sinha, S. K.; Sirota, E. B.; Garoff, S.; Stanley, H. B. *Phys. Rev. B* **1988**, *38*, 2297.

(25) Rowlinson, J. S.; Widom, B. *Molecular Theory of Capillarity*; Clarendon Press: Oxford, 1982.

(26) Weeks, J. D. *J. Chem. Phys.* **1977**, *67*, 3106.

(27) Gelfand, M. P.; Fisher, M. E. *Physica A* **1990**, *166*, 1.

(28) Schlossman, M. L.; Schwartz, D. K.; Kawamoto, E. H.; Kellogg, G. J.; Pershan, P. S.; Kim, M. W.; Chung, T. C. *J. Phys. Chem.* **1991**, *95*, 6628.

(29) Zhang, Y.; Feller, S.; Brooks, B. R.; Pastor, R. W. *J. Chem. Phys.* **1995**, *103*, 10252.

(30) Michael, D.; Benjamin, I. *J. Phys. Chem.* **1995**, *99*, 1530.

(31) Zhang, Z.; Mitrinovic, D. M.; Williams, S. M.; Huang, Z.; Schlossman, M. L. *J. Chem. Phys.* **1999**, in press.

(32) Schlossman, M. L.; Mitrinovic, D. M.; Zhang, Z.; Li, M.; Huang, Z. *Synch. Rad. News* **1999**, in press.